Discrete-ordinates solution of short-pulsed laser transport in two-dimensional turbid media

Zhixiong Guo and Sunil Kumar

The discrete-ordinates method is formulated to solve transient radiative transfer with the incorporation of a transient term in the transfer equation in two-dimensional rectangular enclosures containing absorbing, emitting, and anisotropically scattering media subject to diffuse and/or collimated laser irradiation. The governing equations resulting from the discrete-ordinates discretization of the angular directions are further discretized in the spatial and the temporal domains by the finite-volume approach. The current formulation is suitable for solving transient laser transport in turbid media as well as for steady-state radiative transfer in many engineering problems. The method is applied to several example problems and compared with existing steady-state solutions and Monte Carlo transient solutions. Good agreement is found in all cases. Short-pulsed laser interaction and propagation in a turbid medium with high scattering albedo are studied. The imaging of an inhomogeneous zone inside a turbid medium is demonstrated.

OCIS codes: 030.5620, 140.7090, 000.4430, 170.6920, 170.7050.

1. Introduction

Short-pulsed laser interaction and propagation within turbid media have attracted a great deal of interest in recent years,[1] particularly for applications in biomedical treatment and diagnostics, such as optical tomography, laser surgery, and photodynamic therapy. Fundamental to these laser applications is the determination of transient light distribution in scattering–absorbing media, which influences the rate of heat generation, heat conduction, optothermal properties, and dynamics of ablation.

Modeling of the short-pulsed laser transport has traditionally been done with the diffusion theory. Previously the parabolic diffusion approximation has been widely used for evaluating the reflected and the transmitted intensities of a scattering slab with pulsed irradiation.[2] However, experiments have shown that the diffusion approximation is accurate only for thick samples and fails to match experimental data for thin and intermediate samples.[3] Also, the diffusion model cannot analyze cases with nonscattering or low-scattering regions. Recently several numerical solutions have been developed to simulate time-dependent light transport through absorbing and/or scattering media. One mathematical model for describing short-pulsed laser transport is transient radiative-transfer theory. Complete analytical solutions of the hyperbolic transient radiative-transport equation are not known. Kumar *et al.*[4] considered the solution of transient radiative equation by use of the parabolic and the hyperbolic P_1 models. The adding–doubling method[5,6] was used to solve the transient response of a slab medium and to determine the optical properties of turbid media. More recently, Mitra and Kumar[7] examined several numerical models for short-pulsed laser transport in a one-dimensional planar medium, in which the discrete-ordinates (DO) method, P_N model, diffuse approximation, and two-flux method were addressed. Tan and Hsu[8] developed integral formulation for transient radiative transfer. With the aim of using the radiation element method for irregular geometries, Guo and Kumar[9] extended the radiation element method to consider hyperbolic transient radiative transfer.

Only a few studies have been devoted to multidimensional problems and complex geometries. Yamada and Hasegawa[10] used the finite-element method to solve the parabolic diffusion approximation in two-dimensional (2D) cylindrical media. Mitra *et al.*[11] applied the hyperbolic P_1 model to transient radiative transfer in a 2D rectangular me-

The authors are with the Department of Mechanical, Aerospace, and Manufacturing Engineering, Polytechnic University, 6 Metrotech Center, Brooklyn, New York 11201. S. Kumar's e-mail address is skumar@duke.poly.edu.

Received 18 September 2000; revised manuscript received 19 March 2001.

0003-6935/01/193156-08$15.00/0

dium. Wu and Wu[12] solved the integral equation, using the quadrature method in the study of transient radiative transfer in 2D cylindrical linearly anisotropically scattering media with pulse irradiation.

However, the Monte Carlo (MC) method is always broadly used in the study of laser propagation because of its simple algorithm and flexibility to include real physical conditions. Wilson and Adam[13] developed a MC model to study the propagation of light in tissue. Flock *et al.*[14] tested the MC results by comparison with the diffusion theory. Brewster and Yamada[15] compared measurements with diffusion theory predictions and MC simulations. Guo *et al.*[16] investigated the characteristics of Gaussian temporally and spatially profiled laser transport in multidimensional media. However, the MC method is time consuming, and the results are subject to statistical error resulting from practical finite samplings. Even with a huge sampling number, it is hard to obtain precise radiative fields in fine space and time resolutions with the MC method. In contrast, deterministic methods do not experience these kinds of defects. Among the deterministic methods that have been used to solve multidimensional hyperbolic transient radiative equations, however, the P_1 method dramatically underestimates the light-propagation speed,[7] and the integral formulation[8] is difficult to apply to inhomogeneous and highly anisotropically scattering media.

The DO method has been one of the most widely applied methods for the prediction of multidimensional steady-state radiative transfer in participating media.[17–19] It has also been extensively developed for neutron transport processes.[20] The DO method requires a single formulation for invoking higher-order approximations of DO quadrature sets; it integrates easily into control volume transport codes and is applicable to the complete anisotropic scattering phase function and inhomogeneous media. On the basis of these characteristics, the DO method was selected in this study for implementation into transient radiation transport. A literature survey reveals that the DO method has not, to our knowledge, been formulated for analyzing transient laser transport in a multidimensional medium.

In the present study the DO method is formulated for transient radiative transfer in anisotropically scattering, absorbing, and emitting media in a 2D rectangular enclosure. The transient solutions are compared with existing steady-state solutions for purely absorbing and/or purely scattering media. The transient DO method is examined by comparison with the MC prediction in a transient radiative-heat-transfer problem. The influences of time step and mesh divisions are examined. Finally, the transient DO method is applied to predict short-pulsed laser transport in a scattering-dominated turbid medium with properties similar to those of living tissue. The spatial and the temporal resolutions are as fine as 0.1 mm and 0.1 ps, respectively, so that the fields of transmittance, reflectance, incident radiation, and heat-generation rate are obtained with high resolution. The characteristics of the transient incident radiation inside the medium are discussed. The influences of the absorption coefficient and the optical-fiber location on the temporal reflectance distribution are examined. The imaging of a small inhomogeneous zone inside a turbid medium through the comparison of temporal transmittance is demonstrated.

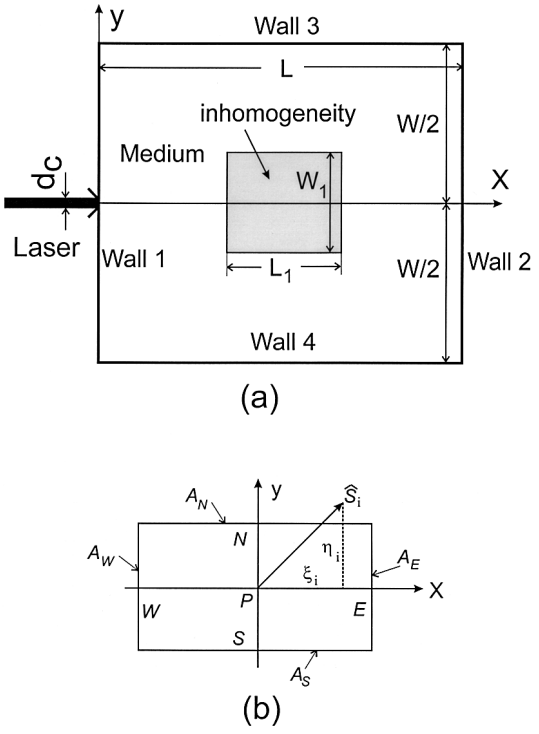

Fig. 1. (a) Sketch of the system, (b) control volume.

2. Mathematical Model

For 2D Cartesian coordinates in a rectangular enclosure, as shown in Fig. 1(a), the transient radiative-transfer equation of intensity I_i in the DO direction $\hat{\mathbf{s}}_i$ can be formulated as

$$\frac{1}{c}\frac{\partial I_i}{\partial t} + \xi_i \frac{\partial I_i}{\partial x} + \eta_i \frac{\partial I_i}{\partial y} + \beta I_i = \beta S_i, \quad i = 1, 2, \ldots, n, \quad (1)$$

where the extinction coefficient β is the sum of the absorption coefficient κ and the scattering coefficient σ; c is light speed in the medium; and S_i is the radiative source term,

$$S_i = (1 - \omega) I_b + \frac{\omega}{4\pi} \sum_{j=1}^{n} w_j \Phi_{ij} I_j + S_c, \quad i = 1, 2, \ldots, n, \quad (2)$$

where scattering albedo $\omega = \sigma/\beta$, Φ_{ij} represents scattering phase function $\Phi(\hat{\mathbf{s}}_j \rightarrow \hat{\mathbf{s}}_i)$, and S_c is the source contribution of collimated irradiation. A quadra-

Table 1. C_k, Expansion Coefficient Values for the Phase Functions

k	PF1	PF2
0	1.00000	1.00000
1	2.00917	0.55355
2	1.56339	0.56005
3	0.67407	0.11572
4	0.22215	0.01078
5	0.04725	0.00058
6	0.00671	0.00002
7	0.00068	
8	0.00005	

ture of order n with the appropriate angular weight w_j is used in the DO method. The scattering phase function may be approximated by a finite series of Legendre polynomials as

$$\Phi_{ij} = \sum_{k=0}^{M} C_k P_k(\cos \phi), \tag{3}$$

and the argument can be obtained as

$$\cos \phi = \hat{\mathbf{s}}_i \cdot \hat{\mathbf{s}}_j = \xi_i \xi_j + \eta_i \eta_j + \mu_i \mu_j. \tag{4}$$

C_k are the expansion coefficients of the corresponding Legendre functions P_k. ξ_i, η_i, and μ_i are the three direction cosines of the DO direction $\hat{\mathbf{s}}_i$. The values of expansion coefficient for phase functions selected in the present study are listed in Table 1.

The enclosure walls are gray and diffusely reflecting. The diffuse intensity at wall 1 is

$$I_w = \epsilon_w I_{bw} + \frac{1 - \epsilon_w}{\pi} \sum_{\xi_j<0}^{n/2} w_j I_j |\xi_j|. \tag{5}$$

Similarly, we can set up relations for three other walls. The details about the treatment of boundary conditions can be found in the literature.[17,19,21]

The collimated laser sheet is normally incident upon the center of wall 1 with a width of d_c. The collimated intensity in the medium within the range of $y \subset (-d_c/2, d_c/2)$ can then be calculated as

$$I_c(x, \xi_c, t) = I_0 \exp(-\beta x)[H(t - x/c) - H(t - t_p - x/c)]\delta(\xi_c - 1), \tag{6}$$

where $H(t)$ and δ are the Heaviside and the Dirac delta functions, respectively, and t_p and I_0 are the pulse width and incident intensity of the ON–OFF square laser pulse. The collimated component S_c in Eq. (2) is then written as

$$S_c = (\omega/4\pi) I_c \Phi(\xi_c \xi_i + \eta_c \eta_i + \mu_c \mu_i), \tag{7}$$

where $\xi_c = 1$, $\eta_c = 0$, and $\mu_c = 0$ in the current study. In the region where no collimated laser irradiation is passing through, $I_c = S_c = 0$.

Once the intensity field is obtained, the incident radiation G and the net radiative heat fluxes Q_x and Q_y can be attained as

$$G = \sum_{j=1}^{n} w_j I_j + I_c, \tag{8}$$

$$Q_x = \sum_{j=1}^{n} \xi_j w_j I_j + I_c, \tag{9}$$

$$Q_y = \sum_{j=1}^{n} \eta_j w_j I_j. \tag{10}$$

If the divergence of the total heat flux is desired, we have

$$\nabla \cdot \mathbf{q} = \kappa(4E_b - G), \tag{11}$$

where E_b is the blackbody radiative emissive power of the medium. For a nonemitting medium such as in the case of short-pulsed laser radiation transport in which the emission term can be neglected because of a cold medium, $E_b = 0$. So the radiative-heat divergence field can easily be obtained from the radiation field.

The transient transmittance at wall 2 and reflectance at wall 1 for scattering–absorbing media exposed to laser irradiation at wall 1 are defined as

$$T(y, t) = \frac{Q_x(x = L, y, t)}{I_0},$$

$$R(y, t) = \frac{Q_x(x = 0, y, t) - I_c(x = 0, y, t)}{I_0}. \tag{12}$$

3. Numerical Solution

To solve the DO Eq. (1), the finite-volume approach is employed. The enclosure is divided into small control volumes by $M_x \times M_y$ meshes. In each control volume, as shown in Fig. 1(b), the spatially and temporally discretized equation can be expressed as

$$(V/c\Delta t)(I_{Pi} - I_{Pi}^0) + \xi_i(A_E I_{Ei} - A_W I_{Wi}) + \eta_i(A_N I_{Ni} - A_S I_{Si}) = \beta V(-I_{Pi} + S_{Pi}), \tag{13}$$

where subscript i is the index of angular discretization; subscript P represents the node of a control volume; subscripts E, W, S, and N stand for the east, west, south, and north faces of the control volume, respectively; I_{Pi}^0 is the intensity at previous time step; S_{Pi} is the radiative source term at node P; A is the area of the face; and V is the volume of the control volume. In 2D geometry, $A_E = A_W = \Delta y$, $A_S = A_N = \Delta x$, and $V = \Delta x \Delta y$. The formulation of Eq. (13) can easily be extended to a three-dimensional geometry by addition of another term accounting for the z direction. The first term in Eq. (13) is the discretized form of the transient term in transfer equation (1), and it accounts for the light propagation. The other terms in Eq. (13) are similar to the steady-state formulation and can be found in the corresponding literature of steady-state radiative transfer[17,19,21] or steady-state neutron transport.[20]

To solve Eq. (13), the weighted diamond differencing scheme has often been introduced[17–21]:

$$I_{Pi} = \gamma_y I_{Ni} + (1 - \gamma_y) I_{Si} = \gamma_x I_{Ei} + (1 - \gamma_x) I_{Wi}. \quad (14)$$

Many types of spatial differencing scheme have been discussed by many researchers for determining the values of γ_x and γ_y. In the present study the positive scheme, which was proposed by Lathrop,[20] is applied.

The final discretization equation for the cell intensity in a generalized form becomes

$$I_{Pi} = \frac{\dfrac{1}{\beta c \Delta t} I_{Pi}^0 + S_{Pi} + \dfrac{|\xi_i|}{\gamma_x \beta \Delta x} I_{xi} + \dfrac{|\eta_i|}{\gamma_y \beta \Delta y} I_{yi}}{\dfrac{1}{\beta c \Delta t} + 1 + \dfrac{|\xi_i|}{\gamma_x \beta \Delta x} + \dfrac{|\eta_i|}{\gamma_y \beta \Delta y}}, \quad (15)$$

where I_{xi} is the x-direction face intensity where the beam enters ($=I_{Wi}$ for $\xi_i > 0$, and $=I_{Ei}$ for $\xi_i < 0$) and I_{yi} is the corresponding y-direction face intensity. The derivation of Eq. (15) is well described by Modest[21] and Kim and Lee[19] for steady-state transfer. In the current study the two Δt-related terms have been derived and added. The derivation of those two Δt-related terms in Eq. (15) follows in a straightforward manner from Eq. (13). Furthermore, in the limiting case in which the time step Δt is infinitely large, Eq. (15) asymptotes to the steady-state form. So the present formulation is feasible for both transient and steady-state radiation transfer. It is worth noting that, even though the present formulation is for 2D geometry, formulation for the three-dimensional case is only a simple extension of the present method with the addition of discretized terms in the third z coordinate. The terms corresponding to the z coordinate are analogous to the discretized terms in the x and the y coordinates.

The solution of the transient radiative field is based on the advancement of time steps. An initial field of intensity is specified on the basis of physical reality. In the present study the initial values of intensity at all discrete ordinates everywhere in the field are set equal to zero. The boundary conditions are given for all directions pointing away from the surface. The solution procedure is similar to the iterative solution used in steady-state transfer as described by Modest.[21] The differences in the present transient solution are (i) the boundary conditions are time dependent, (ii) the iteration is substituted by time advancing, and (iii) the properties of the medium may be time dependent. The present solution is also suitable for obtaining radiative-transfer solutions for steady-state problems. It is worth mentioning that, when the transient solution is used to solve a steady-state problem, the transient solution is expected to be more stable than the iterative steady-state solution. This feature is just like the transient computational fluid dynamics (CFD) scheme.

False numerical diffusion is introduced in the solution, owing to the finite discretizations in space and in time in Eq. (13). To eliminate the numerical diffusion, the space and the time steps are required to be as fine as possible. Consequently, the CPU time will increase. There should be a compromise between computation cost and solution improvement by selection of finer space and time grids. Fiveland[17] showed that the spatial differential step should satisfy the following limitation:

$$\Delta x < |\xi_i|_{\min}/\beta(1 - \gamma_x), \qquad \Delta y < |\eta_i|_{\min}/\beta(1 - \gamma_y). \quad (16)$$

For transient radiative transfer, in addition to inequality (16), a limitation on time step should also be imposed. Since a light beam always travels in a velocity c corresponding to the speed of light in the medium, the traveling distance $c\Delta t$ between two neighboring time steps should not exceed the control volume spatial step, i.e., $c\Delta t < \text{Min}\{\Delta x, \Delta y\}$. Thus, if we introduce the nondimensional time variable $t^* = \beta c t$, we have

$$\Delta t^* < \text{Min}\left\{\frac{|\xi_i|}{1 - \gamma_x}, \frac{|\eta_i|}{1 - \gamma_y}\right\}. \quad (17)$$

It is worth noting that the source term S_{Pi} in Eq. (15) is computed from the latest known intensity values by use of Eqs. (2) and (7), so it is a mixed scheme of current and previous time steps. Therefore the numerical scheme for time discretization is not fully implicit.

The choice of quadrature scheme in the DO method is arbitrary. In the present calculations the S–12 approximation ($n = 84$, which computes 84 fluxes over the hemisphere) is used. The values of DO quadrature sets and weights can be found in Table 2 of Fiveland.[18] The S–12 accuracy in dealing with the anisotropic scattering phase function was also checked by Fiveland.[18] For highly anisotropic phase functions a higher-order S–N approximation should give better results. However, a higher-order approximation requires finer control volume meshes and finer time step. Consequently, the computation becomes more prohibitive.

4. Results and Discussion

First, the transient DO method is applied to a square enclosure with cold, black walls and a purely absorbing medium that is suddenly raised to and maintained at an emissive power of unity. The predicted surface-heat fluxes at different time instants for three different absorption coefficients are plotted in Fig. 2 and compared with exact solutions[22] in steady state. It is seen that the heat flux increases as the time proceeds. After $t^* = 5.0$, the transient results show an excellent match with the exact solutions in steady state. The nondimensional positions are defined as $x^* = x/L$ and $y^* = y/W$ in the current paper.

Second, a boundary incident problem in a square enclosure is studied, where wall 1 is suddenly heated and maintained at a hot temperature with unity emissive power, but all other walls and the medium are kept cold. The medium is strong forward anisotropically scattering with nine terms of the Mie phase function PF1 (see Table 1), and the asymmetry factor

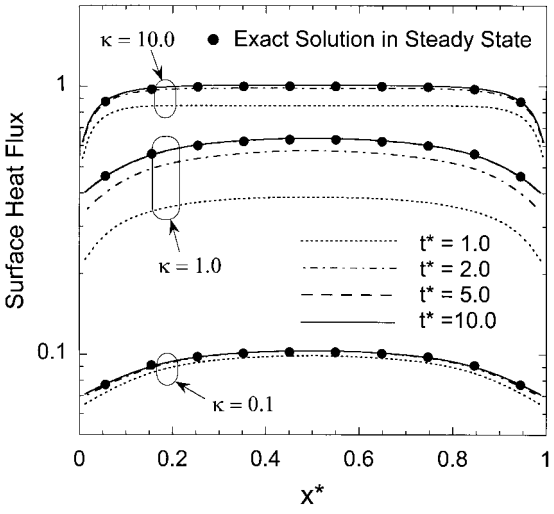

Fig. 2. Transient DO prediction of surface heat flux for a purely absorbing medium and comparison with exact solution.[22]

g is 0.66972. The nondimensional incident radiation and net heat fluxes along the centerline ($y^* = 1/2$) are displayed in Fig. 3 for different time stages. The circles are the values predicted with the steady-state S–14 DO method.[19] As time advances, it is seen that the radiation propagates to the larger x end. The transient results gradually approach the steady-state solutions. The minor difference between the steady-state solution and the transient solution at $t^* = 8.0$ may be attributed to the different-order approximations used in the two solutions.

The transient DO method is again verified by comparison with the MC prediction for an isotropically scattering medium with black walls. Wall 1 is assumed to be hot and irradiated diffusely; other walls and the medium are cold. Other parameters are $L = W = 10$ mm, $\kappa = 0.001$ mm^{-1}, and $\sigma = 1.0$ mm^{-1}.

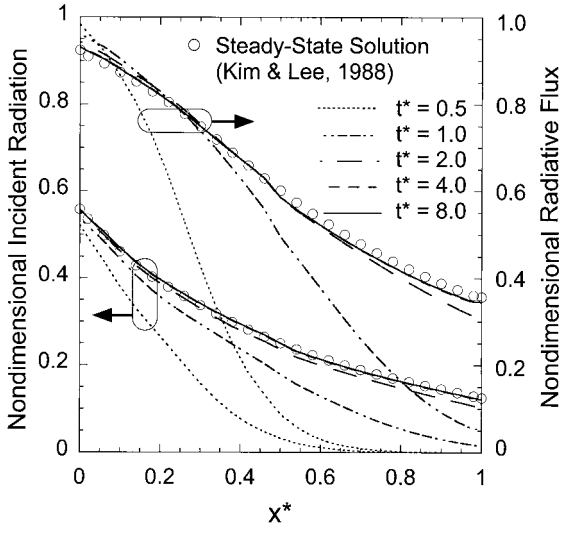

Fig. 3. Transient DO predictions of incident radiation and radiative heat flux for a purely anisotropically scattering medium and comparison with S–14 steady-state solution.[19]

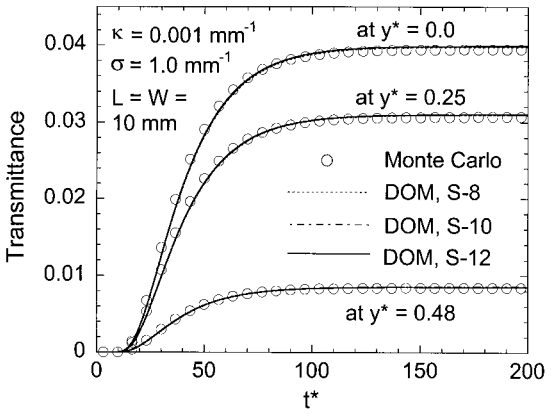

Fig. 4. Comparison of temporal transmittance profiles between DO and MC methods in a square isotropically scattering medium with one hot wall.

The temporal distributions of transmittance at three different locations are shown in Fig. 4. The values of DO sets can be found in a textbook[21] for S–8 approximation and in Fiveland[18] for S–10 approximation. The MC results in the current paper are calculated on the basis of the algorithm developed by Guo *et al.*[16] It is seen that the transient DO results are in excellent agreement with those predicted by the MC method. For an isotropically scattering medium, even a lower-order DO approximation (S–8) can predict accurate results.

The influence of time step in the transient DO method is illustrated in Fig. 5, where the temporal profiles of transmittance at the center of wall 2 are plotted. The geometry of the medium is $L = W = 10$ mm. The medium is anisotropically scattering with phase function PF1 and $\kappa = 0.001$ mm^{-1} and $\sigma = 3.0$ mm^{-1}. Wall 1 is hot and irradiated diffusely; other walls are cold and diffusely reflected with reflectivity $\rho = 0.5$. The equivalent isotropic scattering coefficient is then $\sigma_I = 3.0 \times (1 - g)$ mm^{-1}, and the nondimensional time t_I^* is defined as $(\sigma_I + \kappa)ct$. For

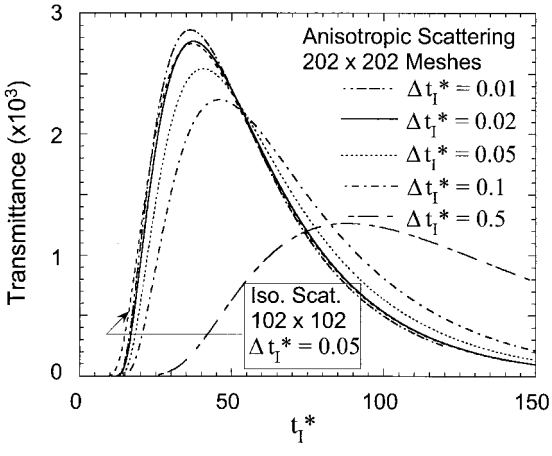

Fig. 5. Influence of time step and comparison of equivalent isotropic scattering results with the direct anisotropic scattering simulations in transient radiation transport.

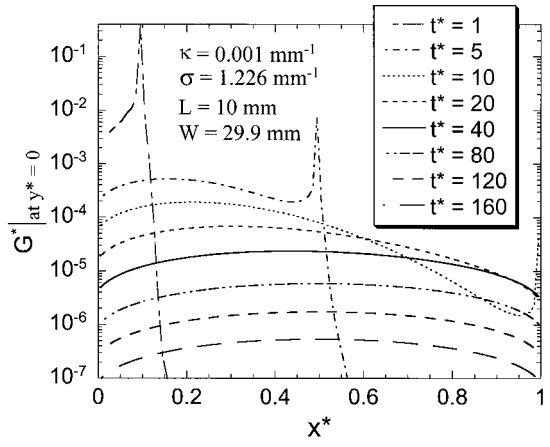

Fig. 6. Nondimensional incident radiation profiles along the centerline at various time instants for a medium subject to ultrashort-pulsed laser irradiation.

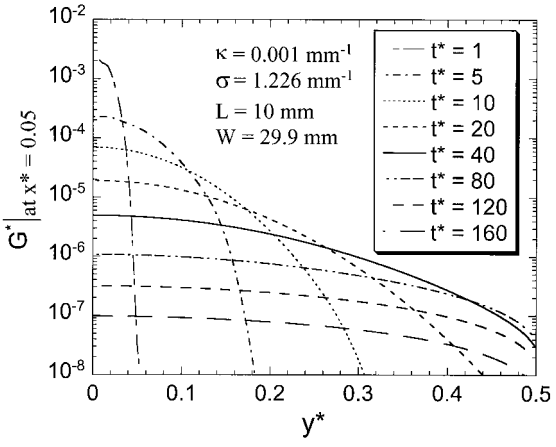

Fig. 7. Nondimensional incident radiation profiles along the y direction near the laser incident surface at various time instants.

anisotropic scattering modeling, the square medium is divided into 202×202 meshes, whereas 102×102 meshes are used for equivalent isotropic scattering modeling. We found that a grid of 102×102 meshes can also predict reasonably accurate temporal transmittance for anisotropic scattering. It is seen that, when inequality (17) is broken ($\Delta t_I^* = 0.5$), the predicted transmittance shape is significantly different from the accurate one because of large numerical diffusion, and the transmitted light is dramatically delayed. As Δt_I^* decreases, the peak position will shift to a shorter time scale, which means that the numerical light-propagation speed will be closer and closer to its real value c. Accurate temporal shape of transmittance can be obtained for anisotropic scattering modeling around $\Delta t_I^* = 0.02$. Since the attenuation coefficient of equivalent isotropic scattering modeling is $\sim 1/3$ that of directly anisotropic scattering modeling, it is seen that the nondimensional time step for isotropic scattering can be two or three times larger than that of corresponding anisotropic scattering. More importantly, it is found that the equivalent isotropic scattering results match closely the Mie phase function anisotropically scattering predictions except at the early time stages. This finding is consistent with our previous finding for a forward-scattering medium with the Henyey–Greenstein phase function.[23]

In Figs. 6–8 ultra-short-pulsed laser transport in a turbid medium is investigated. The enclosure is $L = 10$ mm and $W = 29.9$ mm. The medium properties similar to those of living tissue with refractive index of 1.40, $\kappa = 0.001\ \text{mm}^{-1}$, and $\sigma = 1.226\ \text{mm}^{-1}$. The scattering phase function is PF2 (see Table 1). Internal reflection is not considered, because boundary is matched when the optical fibers are inserted into the body containing the medium. The spatial width of the incident impulse laser is $d_c = 0.1$ mm (to simulate a laser imposed through a 100-μm optical fiber). The control volume size is 0.1 mm $\times$ 0.1 mm to simulate precisely the transient laser transport in fine dimensions and to simulate detectors by use of small optical fibers. The time resolution is $\Delta t = 0.1$ ps. It should be noted that the precise prediction of radiation field at such fine space and time resolutions is of significance in many practical applications, and this is a tough task for MC methods.

Figure 6 shows the nondimensional incident radiation along the centerline ($y^* = 0$) at various time instants. It is clearly seen that the sudden peak, which represents the ballistic component of the laser, propagates from small to large x as time advances, and the peak value is exponentially reduced. The position of the peak is equal to the flight distance of the laser. The diffuse component that is due to multiple scattering also forms a second maximum incident radiation along the x direction. This diffuse peak propagates from the small x to the center of the x axis with a speed much lower than light speed. As time proceeds, the value of the incident radiation becomes increasingly small. At long time stages, the profile of the incident radiation along the x axis is nearly symmetric.

The profiles of nondimensional incident radiation

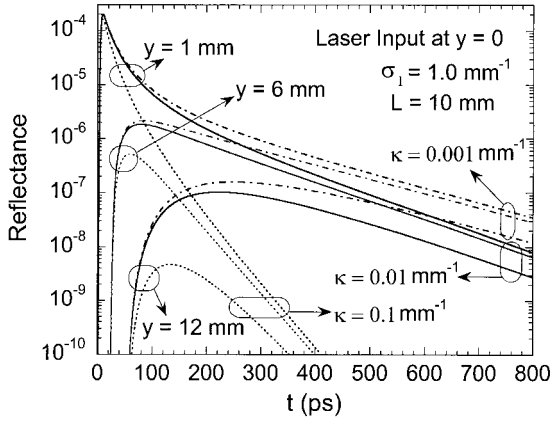

Fig. 8. Influences of absorption coefficient and detector position on the temporal reflectance profiles.

along the y direction at a location near the laser incident surface are demonstrated in Fig. 7 for different time instants. It is seen that the incident radiation is confined in a small region at early time instant ($t^* = 1$). As time increases, the confined region becomes increasingly large, but the magnitude of the intensity becomes smaller and smaller. The incident radiation at the larger y^* position (far from the laser incident point) is always lower than that at the smaller y^* position (near the laser incident point) in the whole transient time domain.

The influence of the absorption coefficient on the temporal reflectance profile is shown in Fig. 8, where three optical-fiber detector positions (y = 1, 6, 12 mm, respectively) are also compared. It is seen that a small increase in the value of the absorption coefficient will result in a corresponding deduction of the reflectance because of the decrease of multiple-scattering events. The logarithmic slope of the reflectance versus the time is different for different absorption coefficients. At long time stages, however, each absorption coefficient corresponds to a logarithmic slope. Hence the slope contains the information of absorption coefficient. When the detector is only 1 mm from the laser incident point (y = 1 mm), the maximum reflectance value and its time position are nearly unchanged for the three different absorption coefficients. However, after passing the peak, the reflectance decreases rapidly for a larger absorption coefficient. When the detector is 12 mm away, however, the magnitude of the reflectance is usually decreased by several orders at early time stages. At long time stages, the difference is $\sim$1 order of magnitude. Generally, the peak reflectance position shifts to small time with the increase of absorption coefficient.

Finally, the imaging of an inhomogeneous zone inside a strongly scattering turbid medium is investigated. The turbid medium is assumed to be in a square enclosure, shown in Fig. 1(a) with $L = W$ = 10.1 mm, $\kappa = 0.01\ \text{mm}^{-1}$, and the reduced scattering coefficient $\sigma_I = 1.0\ \text{mm}^{-1}$. A small inhomogeneous zone is located at the center of the square with $L_1 = W_1 = 1.1$ mm, $\kappa = 0.2\ \text{mm}^{-1}$, and $\sigma_I = 1.2\ \text{mm}^{-1}$. The spatial width of the incident pulse is $d_c = 0.1$ mm, and the pulse duration is 1 ps. The control volume is 0.1 mm $\times$ 0.1 mm, and the time resolution is $\Delta t = 0.1$ ps. It is assumed that there is no change of refractive index between the turbid medium and the inhomogeneous zone. The study is analogous to the imaging of a tumor inside tissues.

The shapes of the logarithmically varied temporal transmittance at different detector locations are compared in Fig. 9 between the homogeneous medium and that with the presence of an inhomogeneous zone at the center. Profile differences between the homogeneous medium and the inhomogeneous one are obvious. At the location (x = 1, y = 0) the transmittance rises at the time $t = 10.1\ \text{mm}/c \approx 47$ ps, which is exactly the shortest flight time of light passing through the medium without interaction with the medium. With or without the inhomogeneity, the earliest rising time does not change. However, after the pulse passes through the medium, the difference of transmittance at the location (1, 0) between the homogenous medium and that with inhomogeneous zone is distinct. The presence of a small inhomogeneity results in a large decrease of the transmittance magnitude. Even if the detector is located at other locations where the direct line between the incident spot and the detector does not pass through the inhomogeneity, such as at (0.75, 0.5) and (1, 0.25), such a decrease is also observable. By detecting the temporal signals at various locations, we can decide the location and size of the inhomogeneity.

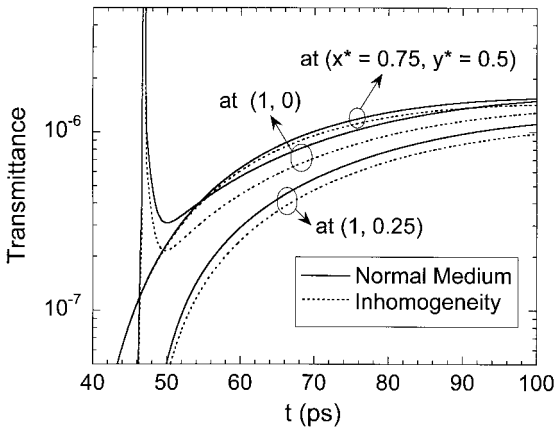

Fig. 9. Comparison of the temporal transmittance profiles at different positions between the homogeneous medium and the medium with a small inhomogeneous zone.

5. Conclusions

The discrete-ordinates (DO) method is developed to study transient radiative transfer in two-dimensional (2D) anisotropically scattering, absorbing, and emitting media subject to diffuse and/or collimate short-pulsed laser irradiation. The transient formulation is feasible for both transient and steady-state radiative transfer. The present solution is verified by comparison with the existing published results and/or with the Monte Carlo (MC) simulation for a variety of example problems. It is found that the present method is accurate and efficient.

The temporal distribution of transmittance in equivalent isotropic scattering modeling is found to match reasonably the predictions of direct modeling of strong forward anisotropic scattering with truncated Legendre polynomials phase function in most of the transient domain except at the regime of early time instants where the isotropic modeling overestimates the transmittance.

The transient DO method is applied to study the characteristics of ultra-short-pulsed laser interaction and propagation within turbid media. It is found that the ballistic component of the laser propagates with the speed of light in the medium, and its value is reduced dramatically with the advance of propagation. The diffuse component that is due to multiple

scattering also forms a second maximum incident radiation inside the medium, and the peak propagates with a speed much lower than the speed of light. A small increase of the absorption coefficient in the medium results in an applicable deduction of the reflectance and transmittance. The broadening shape of the temporal transmittance and reflectance is strongly influenced by the absorption coefficient and the detector location. Differences in the temporal transmittance shape between the homogeneous medium and the medium with an inhomogeneous zone are distinct. The difference is varied according to the relative positions between the inhomogeneous zone, the detector, and the incident laser.

The authors acknowledge partial support from the Sandia–National Science Foundation joint grant AW-9963 administered by Sandia National Laboratories, Albuquerque, New Mexico, where Shawn Burns served as project manager for the grant.

References

1. S. Kumar and K. Mitra, "Microscale aspects of thermal radiation transport and laser applications," Adv. Heat Transfer **33,** 187–294 (1998).
2. M. S. Patterson, B. Chance, and B. C. Wilson, "Time resolved reflectance and transmittance for the noninvasive measurement of tissue optical properties," Appl. Opt. **28,** 2331–2336 (1989).
3. K. M. Yoo, F. Liu, and R. R. Alfano, "When does the diffusion approximation fail to describe photon transport in random media?" Phys. Rev. Lett. **64,** 2647–2650 (1990).
4. S. Kumar, K. Mitra, and Y. Yamada, "Hyperbolic damped-wave models for transient light-pulse propagation in scattering media," Appl. Opt. **35,** 3372–3378 (1996).
5. C. I. Rackmil and R. O. Buckius, "Numerical solution technique for the transient equation of transfer," Numer. Heat Transfer **6,** 135–153 (1983).
6. S. A. Prahl, M. J. C. van Gemert, and A. J. Welch, "Determining the optical properties of turbid media by using the adding–doubling method," Appl. Opt. **32,** 559–568 (1993).
7. K. Mitra and S. Kumar, "Development and comparison of models for light-pulse transport through scattering–absorbing media," Appl. Opt. **38,** 188–196 (1999).
8. Z. M. Tan and P.-F. Hsu, "An integral formulation of transient radiative transfer—theoretical investigation," in *Proceedings of 34th National Heat Transfer Conference* (American Society of Mechanical Engineers, Pittsburgh, Pa., 2000), Paper NHTC2000–12077.
9. Z. Guo and S. Kumar, "Radiation element method for transient hyperbolic radiative transfer in plane–parallel inhomogeneous media," Numer. Heat Transfer B **39,** 371–387 (2001).
10. Y. Yamada and Y. Hasegawa, "Time-dependent FEM analysis of photon migration in biological tissues," JSME Int. J. B **39,** 754–761 (1996).
11. K. Mitra, M.-S. Lai, and S. Kumar, "Transient radiation transport in participating media within a rectangular enclosure," J. Thermophys. Heat Transfer **11,** 409–414 (1997).
12. C.-Y. Wu and S.-H. Wu, "Integral equation formulation for transient radiative transfer in an anisotropically scattering medium," Int. J. Heat Mass Transfer **43,** 2009–2020 (2000).
13. B. C. Wilson and G. Adam, "A Monte Carlo model for the absorption and flux distributions of light tissue," Med. Phys. **10,** 824–830 (1983).
14. S. T. Flock, M. S. Patterson, B. C. Wilson, and D. R. Wyman, "Monte Carlo modelling of light propagation in highly scattering tissues. I. Model predictions and comparison with diffusion theory," IEEE Trans. Biomed. Eng. **36,** 1162–1167 (1989).
15. M. Q. Brewster and Y. Yamada, "Optical properties of thick, turbid media from picosecond time-resolved light scattering measurements," Int. J. Heat Mass Transfer **38,** 2569–2581 (1995).
16. Z. Guo, Z., S. Kumar, and K.-C. San, "Multi-dimensional Monte Carlo simulation of short pulse laser radiation transport in scattering media," J. Thermophys. Heat Transfer **14,** 504–511 (2000).
17. W. A. Fiveland, "Three-dimensional radiative heat transfer solutions by the discrete-ordinates method," J. Thermophys. Heat Transfer **2,** 309–316 (1988).
18. W. A. Fiveland, "The selection of discrete ordinate quadrature sets for anisotropic scattering," ASME Heat Transfer Div. **72,** 89–96 (1991).
19. T. K. Kim and H. Lee, "Effect of anisotropic scattering on radiative heat transfer in two-dimensional rectangular enclosures," Int. J. Heat Mass Transfer **31,** 1711–1721 (1988).
20. K. D. Lathrop, "Spatial differencing of the transport equation: positive vs accuracy," J. Comput. Phys. **4,** 475–498 (1968).
21. M. F. Modest, *Radiative Heat Transfer* (McGraw-Hill, New York, 1993).
22. N. Shah, "New method of computation of radiation heat transfer in combustion chambers," Ph.D. dissertation (Department of Mechanical Engineering, Imperial College of Science and Technology, London, 1979).
23. Z. Guo and S. Kumar, "Equivalent isotropic scattering formulation for transient short-pulse radiative transfer in anisotropic scattering planar media," Appl. Opt. **39,** 4411–4417 (2000).